Prell, W. L., Niitsuma, N., et al., 1991
*Proceedings of the Ocean Drilling Program, Scientific Results*, Vol. 117

# 28. U-SERIES DISEQUILIBRIUM, PARTICLE SCAVENGING, AND SEDIMENT ACCUMULATION DURING THE LATE PLEISTOCENE ON THE OWEN RIDGE, SITE 722[1]

Graham B. Shimmield[2] and Stephen R. Mowbray[2]

**ABSTRACT**

High resolution sampling of the upper 10 m of Hole 722B has provided information on the extent of $^{234}U/^{230}Th$ disequilibrium in Owen Ridge sediments accumulating over the last 250 k.y. High biological productivity in surface waters is sustained by seasonal upwelling driven by the Southwest Monsoon. Evidence from the Owen Ridge suggests that there has been significant variation in this productivity over the late Pleistocene, and that greater biological production occurred during interglacial episodes. The resulting organic matter flux drives a variety of redox-related reactions in the sediment, including the reduction and fixing of U. High precision measurements of U/Th trace the paleoproductivity record of enhanced organic matter input during the interglacials. Sedimentary $^{230}Th$, produced by $^{234}U$ decay in the water column, is a sensitive indicator of water column scavenging by particulates, and sediment winnowing and focusing. The decay-corrected flux of excess $^{230}Th$ at the Owen Ridge is substantially less than that recorded at other upwelling margins. The historical record of $^{230}Th$ flux suggests that erosion and winnowing of fine sediment has occurred at the ridge site by active intermediate water circulation, and that this was most prevalent during mid isotope Stage 5 to Stage 3.

## INTRODUCTION

Under conditions of high biological productivity that occur at continental margins where upwelling is intensified, enhanced particulate scavenging of reactive trace metals and radionuclides is known to be manifest (Bacon et al, 1976; Turekian, 1977; Spencer et al., 1981; DeMaster, 1981; Anderson et al; 1983a, b; Mangini and Diester-Haass, 1983; Shimmield et al; 1986). The high production of biogenic particulate matter, and recycling of redox-sensitive metals through the associated oxygen minimum zone, sustains a substantial flux to the seafloor of the scavenged metals (e.g., Th, Pa, Pb), together with increased diagenetic enrichment of redox-sensitive metals (U, Mo) in the reducing sediment (Veeh, 1967; Yamada and Tsunogai, 1984; Shimmield and Pedersen, in press).

Complete, long records of sediment accumulation under productive continental margin waters record a variety of chemical tracers attributable to variation in productivity and upwelling (Boyle, 1983; Mangini and Diester-Haass, 1983; Shimmield and Mowbray, this volume), but often the chronology of the source function (production history) is poorly constrained. However, disequilibrium within the natural $^{238}U$ decay series is particularly interesting in that the production of particle reactive $^{230}Th$ from dissolved parent $^{234}U$ has remained almost constant over the late Pleistocene due to the long residence time of U in seawater (Ku et al., 1977). As U is found at constant composition and isotopic ratio ($^{234}U/^{238}U = 1.14 \pm 0.01$) in normal salinity waters, it is possible to calculate the theoretical production rate of daughter $^{230}Th$. This isotope is very particle reactive with a short residence time of 41 ± 3 yr (Anderson et al., 1983a) so that radioactive decay within the water column is negligible ($t_{1/2}$ = 75,200 yr). Consequently, $^{230}Th$ possesses unique characteristics as a chemical tracer in that its production rate and theoretical flux to the seafloor is well constrained.

In the northwest Arabian Sea the seasonally-reversing summer Southwest Monsoon sustains active oceanic upwelling and high biological productivity through Ekman transport of the surface waters (Qasim, 1982; Slater and Kroopnick, 1984; Prell, 1984a, b). From several studies of proxy-indicators of upwelling intensity and Monsoon wind strength (pollen type, Van Campo et al., 1982; foraminiferal species, Prell, 1984a, b; stable $\delta^{18}O$ signatures of benthic and planktonic foraminifera, Prell, 1984a, b; Duplessy, 1982; inorganic geochemistry, Shimmield and Mowbray, this volume) the history of the Southwest Monsoon and associated variations in paleoproductivity have been inferred.

In the study presented here we have taken the opportunity of the complete, high resolution record of sedimentation obtained at Site 722 on the Owen Ridge (Fig. 1) to investigate the variation in $^{230}Th$ activity and flux over the last 250 k.y. We compare the observed input of particle reactive $^{230}Th$ to both the theoretical production rate, and to that found in other upwelling areas (northwest Africa, Mangini and Diester-Haass, 1983; Baja California, Shimmield et al., 1986). Our study, the first on $^{234}U/$

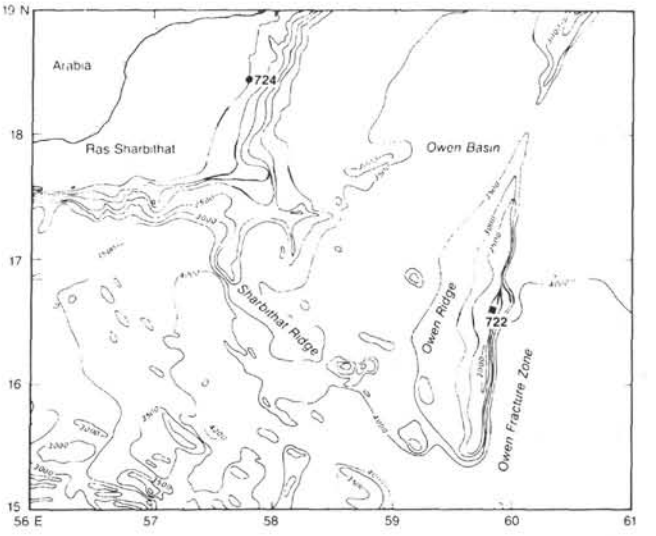


Figure 1. Location of Site 722 in the Northwest Arabian Sea.

[1] Prell, W. L., Niitsuma, N., et al., 1991. *Proc. ODP, Sci. Results*, 117: College Station, TX (Ocean Drilling Program).

[2] Department of Geology and Geophysics, University of Edinburgh, West Mains Road, Edinburgh, EH9 3JW, Scotland, U.K.

$^{230}$Th disequilibrium from the northwest Arabian Sea, suggests that surprisingly low fluxes of excess $^{230}$Th occur and that significant erosion and winnowing of fine material may have occurred on the Owen Ridge. However, the distribution of redox-sensitive U within the sediments appears to record faithfully the inferred variation in productivity at the Oman Margin.

## SAMPLING AND METHODS

Site 722 was selected as an ideal site for high resolution studies of U-series disequilibrium in late Pleistocene sediments as its Owen Ridge top location (2028 m depth) is free from effects of lateral sediment input. In effect, the excess $^{230}$Th activity that we measure here should result from vertical particle scavenging in the overlying water (with possible removal after deposition by bottom currents). In Hole 722B the upper (I) lithologic unit was sampled and is composed of foraminifer-bearing nannofossil ooze (5%–25% foraminifers). On vertical sectioning of the core, 20 $cm^3$ plugs were taken at 20 cm intervals and sealed in polythene bags. Samples were kept at 4°C until processing. Water contents were estimated from weight loss on drying at 60°C. Using an average grain density of 2.6 g $cm^{-3}$ (Shipboard Scientific Party, 1989) dry bulk density values were calculated. Sea salt contribution was obtained assuming a pore water salinity of normal seawater. All data presented in Appendix A are corrected for sea salt dilution.

After drying and grinding to a fine powder the sediments were completely digested in a mixture of HF, $HNO_3$, and $HClO_4$ acids together with a mixed $^{228}$Th/$^{232}$U tracer of known activity. Following di-isopropyl ether extraction of dissolved Fe and ion exchange chromatography under HCl and $HNO_3$ media to separate U and Th isotopes, the nuclides were electro-deposited onto stainless steel planchettes from $(NH_4)SO_4$ media. Estimates of error are given in Appendix B and are calculated from propagated analytical errors and 1$\sigma$ counting errors. All activities are quoted in units of disintegrations per minute per gram dry weight (dpm $g^{-1}$) following standard oceanographic conventions. Data on the concentration of U and Th (in ppm units) are given in Appendix A of Shimmield and Mowbray (this volume) and are calculated from $^{238}$U and $^{232}$Th activities and their relevant isotopic abundance.

## RESULTS

In order to present the U-series data obtained from this study on a geochronological basis, and to correct for ingrowth and decay (see below) of the relevant nuclides, a detailed age model for the late Pleistocene in Hole 722B is required. We are grateful to S. Clemens and W. Prell (see this volume) for providing such an age model based on $\delta^{18}$O stratigraphy of the planktonic foraminifer *G. sacculifer*. Figure 2 presents the uncorrected data for parent $^{234}$U and daughter $^{230}$Th with age (depth in the core) together with 1$\sigma$ error bars. From interpretation of the $\delta^{18}$O stratigraphy the appropriate isotope stages are also indicated. Close examination of the $^{230}$Th profile indicates that the observed activity is generally less than the $^{234}$U parent in the upper (younger) portion of the core sampled, and that with depth (age) the $^{230}$Th approaches secular equilibrium with its parent $^{234}$U. Such a situation in deep-sea sediments is relatively unusual (normally large excesses of daughter $^{230}$Th are observed) and is due to the comparatively shallow water depth and high organic matter flux promoting active U diagenesis. These points are addressed further below. The average uncorrected $^{230}$Th activity of 2–3 dpm $g^{-1}$ appears to be slightly higher in interglacial episodes, and is accompanied by rather greater changes in $^{234}$U activity.

Figure 3 presents the variation between U and Th on a weight ratio basis. Th (calculated from $^{232}$Th activity) is almost exclusively controlled by the detrital noncarbonate phases in the sediment. On the other hand, U is strongly redox sensitive, occurring as a dissolved uranyl carbonate species (+6 oxidation state) in oxygenated seawater, but becomes reduced (+4 oxidation state) and fixed within anaerobic sediments. Since there is often an association between redox state and organic matter content of the sediment, and U is often bound to organic matter (see Shimmield and Pedersen, in press, for review), then the strong agreement between elevated U/Th ratios and productivity indicators (such as Ba/Al) is to be expected (Fig. 3). It is clear that during interglacial episodes there were substantial increases in surface water productivity in the northwest Arabian Sea (see Shimmield and Mowbray, this volume) promoting enhanced flux and accumulation of phytodetritus in the sediments. It is probable that subsequent shallowing of the U redoxcline within the sediment allowed substantial reduced U fixation within the sediment, although variation in sediment accumulation rate is also an important variable. Once U has become fixed, there appears to be little post-depositional remobilization.

The distribution of $^{230}$Th observed in Hole 722B can be attributed to three main sources: (1) detrital $^{230}$Th deposited in equilibrium with parent $^{234}$U, (2) ingrown $^{230}$Th from authigenic $^{234}$U, and (3) excess $^{230}$Th ($^{230}Th_{xs}$) scavenged from the water column (which decays with a half-life of 75,200 yr). In Figure 4 the total $^{230}$Th measured has been corrected for each of these sources (see Appendix A for methods of calculation and further explanation) to obtain an estimate of the initial activity ($A_0$) of $^{230}Th_{xs}$ at the time of deposition. The calculation of initial activity is very sensitive to the estimation of detrital $^{234}$U and $^{230}$Th. Rather than use a global average figure, we have performed radiochemical analysis on surficial samples from 21 box-cores in the northwest Arabian Sea (Shimmield, unpubl. data). Least squares regression of this data set suggests the average initial activity of $^{234}$U is 1.03 × $^{232}$Th activity. Figure 4 indicates that the highest initial activities occur in the Holocene (Stage 1), early Stage 5, and mid-Stage 6. Generally, lower initial activities occur within the glacial sediments. There is a broad correspondence between the $A_0{}^{230}Th_{xs}$ activity and productivity indicators (Ba/Al, Fig. 2) from the beginning of Stage 5 to the present suggesting a link between the activity of the nuclide in the sediment and paleoproductivity. It is the nature of this link, and the modification of the sedimentary record of $^{230}Th_{xs}$ which we discuss in the following section. The lack of correspondence between $A_0{}^{230}$Th and Ba/Al before Stage 5 is due to increased error in the calculation (as $^{230}$Th approaches transient equilibrium with $^{234}$U) and uncertainties in the age model.

## DISCUSSION

The depositional flux of $^{230}Th_{xs}$ ($f$) through time may be calculated from:

$$f = S \cdot A_0{}^{230}Th_{xs} \cdot \rho$$

where S is the linear sediment accumulation rate (cm k.y.$^{-1}$), $A_0{}^{230}Th_{xs}$ is the age corrected initial $^{230}Th_{xs}$ activity (dpm $g^{-1}$) and $\rho$ is the dry bulk density (g $cm^{-3}$). The flux thus calculated is displayed in Figure 5. At Site 722 the expected water column flux of $^{230}Th_{xs}$ is assumed to be equal to its rate of production in the water column from decay of $^{234}$U and therefore depends on the water depth (z). Hence, the predicted flux ($f_{pred}$) is:

$$f_{pred} = 0.00263 \times z$$

giving a value of 5.3 dpm $cm^{-2}$ k.y.$^{-1}$ (shown by vertical dashed line in Fig. 5). It is clear that this flux is exceeded during the Holocene, early Stage 5 and Stage 6, whilst lower-than-predicted fluxes occur from mid-Stage 5 to Stage 3. Clearly, the deposition rate of $^{230}Th_{xs}$ has varied with time.

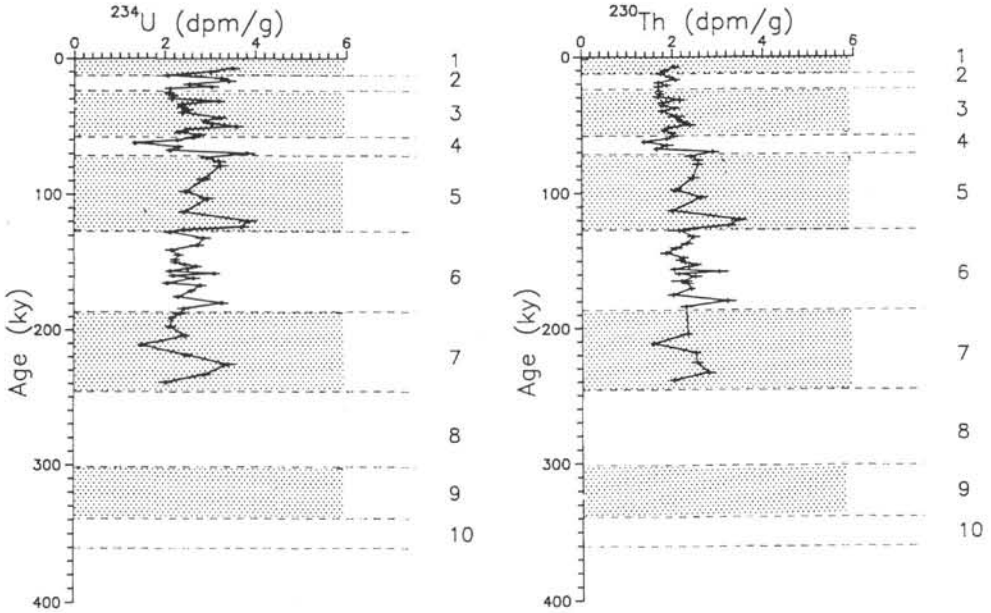


Figure 2. The distribution of $^{234}$U and $^{230}$Th activity (uncorrected except for salt dilution) with age in Hole 722B. The error bars are calculated from 1$\sigma$ counting statistics and propagated analytical uncertainties. The numbered isotope stages are derived from the $\delta^{18}$O stratigraphy of planktonic foraminifers (see Fig. 3).

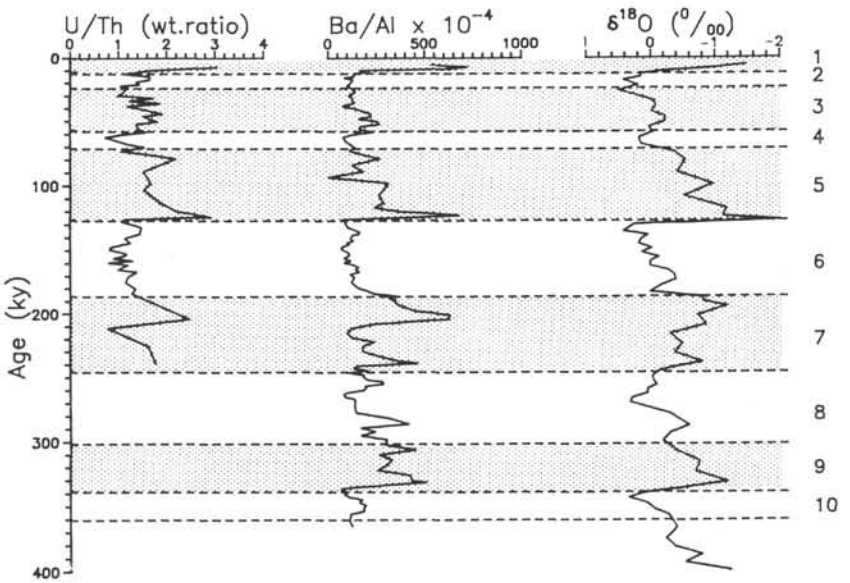


Figure 3. The distribution with time of U/Th (weight ratio), Ba/Al ($\times 10^{-4}$) and $\delta^{18}$O in *G. sacculifer* (Clemens and Prell, this volume).

As described in the introduction, continental margins are known to have high rates of $^{230}$Th scavenging (Anderson et al., 1983b; Mangini and Diester-Haass, 1983; Shimmield et al., 1986). From these studies, and sediment trap work in the Sargasso Sea (Bacon et al., 1985), we can compare the results from Hole 722B with areas identified as important sinks for $^{230}$Th (Fig. 6). Interestingly, although there is a significant positive correlation between sediment accumulation rate and $A_0{}^{230}Th_{xs}$ flux at Site 722, the magnitude of the flux for a given accumulation rate is less than that observed off northwest Africa (Mangini and Diester-Haass, 1983) and much less than that off Baja California (Shimmield et al., 1986), even accounting for the deeper water depths at these localities (see Fig. 6).

As can be seen in Figure 5, a significant proportion of the measured $^{230}Th_{xs}$ flux is in deficit when compared to water column production rates. We suggest that the generally low $^{230}Th_{xs}$ fluxes and the marked deficit from Stage 5 to Stage 3 are a result of winnowing and current erosion removing the fine fraction of the sediment. Cochran and Osmond (1976) identified sediment redistribution patterns in the Tasman Basin where excesses of $^{230}$Th occurred in the basins and deficits on the ridges, but gave an overall balance of the $^{230}$Th flux for the basin. More recently

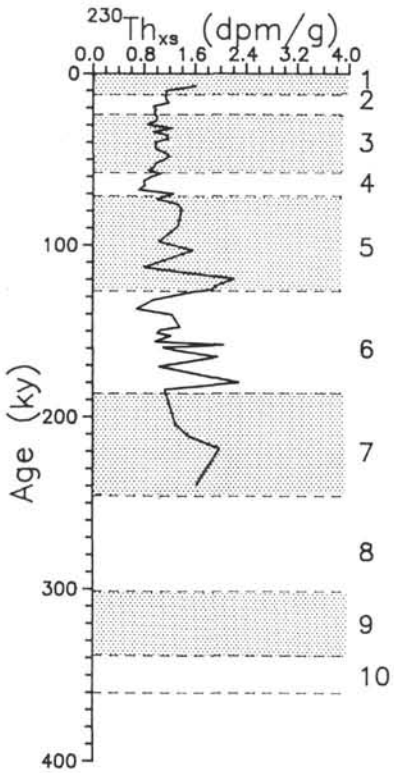


Figure 4. The age distribution of excess $^{230}Th$ corrected for detrital component, ingrowth from parent authigenic $^{234}U$, and radioactive decay (see Appendix A for details of calculation) in Hole 722B, measured in dpm $g^{-1}$.

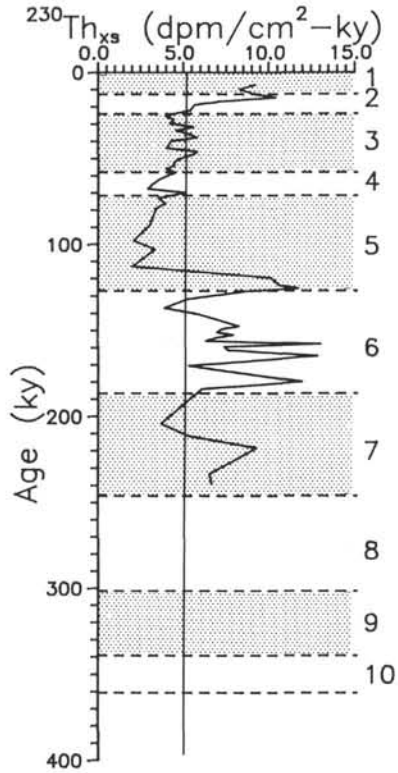


Figure 5. The flux of $^{230}Th_{xs}$ (dpm $cm^{-2}$ k.y.$^{-1}$) with time in Hole 722B. See text for details of flux calculation. The vertical line represents the present day expected flux of 5.3 dpm $cm^{-2}$ k.y.$^{-1}$.

Mangini et al. (1987) and Mangini and Kuhnel (1987) have identified erosion events from the Pacific (Peru Basin and Clarion-Clipperton fracture zone, respectively). In both studies they attribute the enhanced deep water circulation to "periods of climatic change, representing both climatic amelioration and deterioration" occurring at 11, 70–79, 117–127, and 173–193 k.y.BP in the Pacific. At Site 722 the stratigraphy of these erosion events is dissimilar, although the Owen Ridge site will be subject to changes in Indian Ocean Intermediate Water flow rather than Antarctic Bottom Water suggested by Mangini and co-workers. In another study in this volume (Clemens and Prell, 1990) it is apparent that rather different late Pleistocene accumulation rates exist between ridge sites. They indicate that sedimentation at Site 722 is some 25% higher than at an adjacent ridge site sampled by piston core RC27-61. Nevertheless, chemical ($CaCO_3$ wt.%) and grain size variation are preserved between the two cores. They suggest that the strong, coherent eolian depositional signal is preserved despite fine fraction winnowing. We suggest that winnowing is also present at Site 722. Clearly, the $^{230}Th_{xs}$ activity calculated will have been modified by this winnowing, masking the productivity signal attributable to enhanced particle scavenging. We have studied other box and piston cores collected from a previous cruise to the Oman Margin in order to construct a regional history of $^{230}Th$ scavenging at the Oman Margin (Shimmield, unpubl. data). Nevertheless, the paleoredox signal (identified from the U/Th ratio) is preserved and closely correlates with other indicators of paleoproductivity (Fig. 3; Shimmield and Mowbray, this volume). This is probably due to the diagenetic process of U fixation in the more organic-rich sediments, rather than scavenging onto fine particles in the water column which can be easily transported away by bottom currents.

## CONCLUSION

Sediments collected from the crest of the Owen Ridge at Site 722 record 250 k.y. of $^{234}U$ and $^{230}Th$ flux variation. During periods of high biological productivity in surface waters (interglacial episodes) substantial fluxes of biogenic fallout occurred and may be traced within the sediment record (see Shimmield and Mowbray, this volume). Comparison of the U/Th ratio, measured by $\alpha$-spectrometry, with indicators of paleoproductivity (Ba/Al) clearly indicate that enrichment of redox-sensitive U occurs in the more organic-rich sediment. The U is reduced (from 6+ oxidation state to 4+ state) and fixed within the sediment by diagenetic processes, preserving a paleoredox signal over the late Pleistocene.

From measurements of $^{230}Th$, and estimation of detrital contribution, ingrowth from authigenic $^{234}U$, and decay of initial unsupported $^{230}Th$, the past record of $^{230}Th_{xs}$ has been established (using $\delta^{18}O$ stratigraphy from planktonic foraminifers). From the estimate of $^{230}Th_{xs}$ flux, and comparison with flux measurements from other highly productive upwelling areas (northwest Africa, Baja California), it is apparent that the expected high $^{230}Th_{xs}$ flux to the Owen Ridge site is not found. Comparison with expected production from the overlying 2028 m water column suggests that the paleoproductivity signal of $^{230}Th_{xs}$ (caused by intensified particle scavenging) is modified by erosion and winnowing. We suggest that particularly enhanced intermediate water circulation from mid-Stage 5 to Stage 3 can be identified. This hypothesis remains to be confirmed by detailed grain-size analysis. At Site 722 the late Pleistocene sedi-

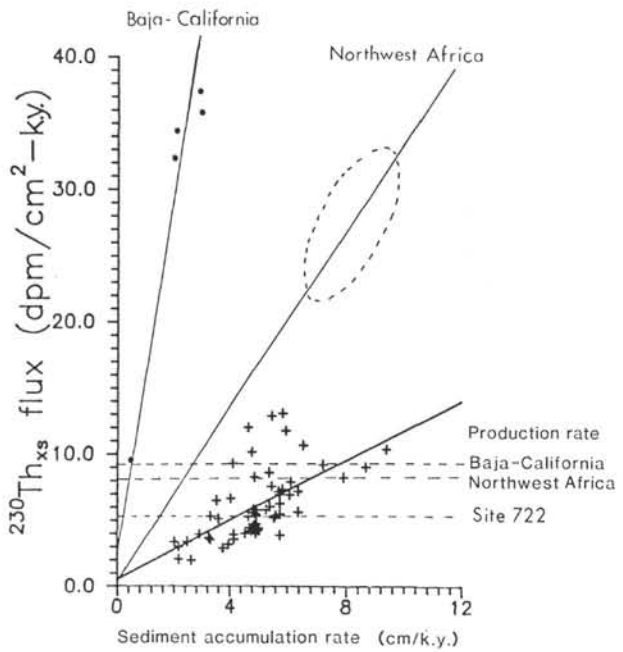


Figure 6. A plot of measured $^{230}Th_{xs}$ flux (dpm cm$^{-2}$ k.y.$^{-1}$) against sediment accumulation rate (cm k.y.$^{-1}$, derived from $\delta^{18}O$ stratigraphy of planktonic foraminifers) in Hole 722B (crosses). Also shown are the data from Baja California (dots, Shimmield et al., 1986) and the regression line and approximate field of data for glacial sediment off northwest Africa (Mangini and Diester-Haass, 1983). The dashed horizontal lines represent the water column production rates for the three areas. Site 722 clearly has lower $^{230}Th_{xs}$ fluxes than the other two upwelling areas.

ment accumulation rate is lower than at other Owen Ridge sites due to this current winnowing.

## ACKNOWLEDGMENTS

We wish to thank the staff and crew of the Ocean Drilling Program and the *JOIDES Resolution* for the opportunity to undertake this study. We are especially grateful to Warren Prell, Kay Emeis, Brian Price, Tom Pedersen, and Steve Clemens for helpful discussions on this project. Dr. R. Anderson and an anonymous reviewer provided helpful comments on this manuscript. GBS acknowledges the support of NERC Grant GST/02/315 from the ODP Special Topic fund.

## REFERENCES

Anderson, R. F., Bacon, M. P., and Brewer, P. G., 1983a. Removal of $^{230}Th$ and $^{231}Pa$ from the open ocean. *Earth Planet. Sci. Lett.*, 62:7–23.

_____, 1983b. Removal of $^{230}Th$ and $^{231}Pa$ at ocean margins. *Earth Planet. Sci. Lett.*, 66:73–90.

Bacon, M. P., Huh, C.-A., Fleer, A. P., and Deuser, W. G., 1985. Seasonality in the flux of natural radionuclides and plutonium in the deep Sargasso Sea. *Deep-Sea Res. Part A*, 32:273–286.

Bacon, M. P., Spencer, D. W., and Brewer, P. G., 1976. $^{210}Pb/^{226}Ra$ and $^{210}Po/^{210}Pb$ disequilibria in seawater and suspended particulate matter. *Earth Planet. Sci. Lett.*, 32:277–296.

Boyle, E. A., 1983. Chemical accumulation variations under the Peru Current during the past 130,000 years. *J. Geophys. Res.*, 88:7667–7680.

Clemens, S. C., and Prell, W. L., 1990. Late Pleistocene variability of Arabian Sea summer-monsoon winds and dust source-area aridity: an eolian record from the lithogenic component of deep-sea sediments. *Paleoceanography*, 5:109–145.

Cochran, J. K., and Osmond, J. K., 1976. Sedimentation patterns and accumulation rates in the Tasman Basin. *Deep-Sea Res. Oceanogr. Abstr.*, 23:193–210.

DeMaster, D. J., 1981. The supply and accumulation of silica in the marine environment. *Geochim. Cosmochim. Acta*, 45:1715–1732.

Duplessy, J. C., 1982. Glacial to interglacial contrasts in the northern Indian Ocean. *Nature*, 295:494–498.

Ku, T.-L., Knauss, K. G., and Mathieu, G. G., 1977. Uranium in open ocean: concentration and isotope composition. *Deep-Sea Res. Oceanogr. Abstr.*, 24:1005–1017.

Mangini, A., and Diester-Haass, L., 1983. Excess Th-230 in sediments off northwest Africa traces upwelling in the past. *In* Suess, E., and Thiede, J. (Eds.), *Coastal Upwelling, its Sediment Record*: New York (Plenum), 455–471.

Mangini, A., and Kuhnel, U., 1987. Depositional history in the Clarion-Clipperton Zone during the last 250,000 years—$^{230}Th$ and $^{231}Pa$ methods. *Geol. Jahrb.*, D87:105–121.

Mangini, A., Stoffers, P., and Botz, R., 1987. Periodic events of bottom transport of Peru Basin sediment during the Late Quaternary. *Mar. Geol.*, 76:325–329.

Prell, W. L., 1984a. Monsoonal climate of the Arabian Sea during the late Quaternary: a response to changing solar radiation. *In* Berger, A. L., Imbrie, J., Hays, J., Kukla, G., and Saltzman, B. (Eds.). *Milankovitch and Climate* (Pt. 1): Dordrecht (D. Reidel), 349–366.

_____, 1984b. Variation of monsoonal upwelling: a response to changing solar radiation. *In* Hansen, J. E., and Takahashi, T. (Eds.), *Climatic Processes and Climate Sensitivity*. Am. Geophys. Union, Maurice Ewing Series, 5:48–57.

Quasim, S. Z., 1982. Oceanography of the northern Arabian Sea. *Deep-Sea Res. Part A*, 29:1041–1068.

Shimmield, G. B., Murray, J. W., Thomson, J., Bacon, M. P., Anderson, R. F., and Price, N. B., 1986. The distribution and behaviour of $^{230}Th$ and $^{231}Pa$ at an ocean margin, Baja California, Mexico. *Geochim. Cosmochim. Acta*, 50:2499–2507.

Shimmield, G. B., and Pedersen, T. F., in press. The geochemistry of reactive trace metals and halogens in hemipelagic continental margin sediments. *CRC Crit. Rev. Mar. Sci.*

Shipboard Scientific Party, 1989. Site 722. *In* Prell, W. L., Niitsuma, N., et al., *Proc. ODP, Init. Repts.*, 117: College Station, TX (Ocean Drilling Program), 255–318.

Slater, R. D., and Kroopnick, P., 1984. Controls on dissolved oxygen distribution and organic carbon deposition in the Arabian Sea. *In* Haq, B. U., and Milliman, J. D. (Eds.), *Marine Geology and Oceanography of Arabian Sea and Coastal Pakistan*. New York (Van Nostrand Reinhold), 305–313.

Spencer, D. W., Bacon, M. P., and Brewer, P. G., 1981. Models of the distribution of $^{210}Pb$ in a section across the north equatorial Atlantic Ocean. *J. Mar. Res.*, 39:119–138.

Turekian, K. K., 1977. The fate of metals in the oceans. *Geochim. Cosmochim. Acta*, 41:1139–1144.

Van Campo, E., Duplessy, J. C., and Rossignol-Strict, M., 1982. Climatic conditions deduced from a 150-kyr oxygen isotope-pollen record from the Arabian Sea. *Nature*, 296:56–59.

Veeh, H. H., 1967. Deposition of uranium from the ocean. *Earth Planet. Sci. Lett.*, 3:145–150.

Yamada, M., and Tsunogai, S., 1984. Postdepositional enrichment of uranium in sediment from the Bering Sea. *Mar. Geol.*, 54:263–276.

**Date of initial receipt: 27 September 1989**
**Date of acceptance: 13 April 1990**
**Ms 117B-169**

## APPENDIX A

Calculation of initial excess $^{230}Th$ activities

1. Correct all activity data for salt dilution.
2. Calculate detrital $^{230}Th$ activity: Assume $^{230}Th$ is in equilibrium with detrital parent $^{234}U$. From multiple regression of box-core core top data (Shimmield, unpubl. data) from the Oman Margin with $^{234}U/^{238}U$ ratios = 1.0 ± 0.05,

$$^{234}U_{detrital} = 1.03 \cdot {}^{232}Th$$

(All $^{232}Th$ is assumed to be detrital). Hence,

$$^{230}Th_{detrital} = {}^{234}U_{detrital}$$

3. Calculate ingrowth from authigenic $^{234}U$ parent:

$$^{230}Th_{ingrown} = {}^{234}U_{authigenic} \cdot (1 - e^{-\lambda t})$$

$$\text{i.e., } {}^{230}Th_{ingrown} = ({}^{234}U_{total} - {}^{234}U_{detrital}) \cdot (1 - e^{-0.009217\,t})$$

4. Calculate initial excess $^{230}Th$:

$$A_0{}^{230}Th_{xs} = \frac{{}^{230}Th_{total} - ({}^{230}Th_{ingrown} + {}^{230}Th_{detrital})}{e^{-0.009217\,t}}$$

Where: all isotopes are expressed in activity units (dpm $g^{-1}$)
$\lambda$ is the $^{230}Th$ decay constant ($^{-k.y.}$)
t is the age of the sample (k.y.)

## APPENDIX B

**Cores 722B-1H and-2H, corrected for salt contribution and dilution.**

| Core, section, interval (cm) | Depth (mbsf) | [a]Age (k.y.) | $^{238}U$ (dpm $g^{-1}$) | ± | $^{234}U$ (dpm $g^{-1}$) | ± | $^{232}Th$ (dpm $g^{-1}$) | ± | $^{230}Th$ (dpm $g^{-1}$) | ± |
|---|---|---|---|---|---|---|---|---|---|---|
| 117-722B- | | | | | | | | | | |
| 1H-1, 6–8 | 0.07 | 6.0 | 3.084 | 0.140 | 3.486 | 0.156 | 0.337 | 0.027 | 2.052 | 0.100 |
| 1H-1, 16–18 | 0.17 | 7.5 | — | — | — | — | — | — | — | — |
| 1H-1, 26–28 | 0.27 | 9.0 | 2.684 | 0.126 | 3.000 | 0.139 | 0.554 | 0.037 | 1.831 | 0.091 |
| 1H-1, 36–38 | 0.37 | 10.2 | — | — | — | — | — | — | — | — |
| 1H-1, 46–48 | 0.47 | 11.5 | 1.901 | 0.101 | 2.058 | 0.108 | 0.554 | 0.038 | 1.737 | 0.088 |
| 1H-1, 56–58 | 0.57 | 12.8 | — | — | — | — | — | — | — | — |
| 1H-1, 66–68 | 0.67 | 14.0 | 2.893 | 0.133 | 3.235 | 0.147 | 0.580 | 0.039 | 1.933 | 0.096 |
| 1H-1, 76–78 | 0.77 | 15.0 | — | — | — | — | — | — | — | — |
| 1H-1, 86–88 | 0.87 | 16.1 | 3.142 | 0.153 | 3.402 | 0.164 | 0.630 | 0.046 | 2.062 | 0.109 |
| 1H-1, 96–98 | 0.97 | 17.2 | 2.371 | 0.122 | 2.534 | 0.129 | 0.575 | 0.044 | 1.691 | 0.093 |
| 1H-1, 106–108 | 1.07 | 19.2 | 2.656 | 0.141 | 3.018 | 0.157 | 0.616 | 0.045 | 1.869 | 0.099 |
| 1H-1, 116–118 | 1.17 | 21.2 | 1.904 | 0.103 | 2.103 | 0.111 | 0.611 | 0.046 | 1.677 | 0.093 |
| 1H-1, 126–128 | 1.27 | 22.3 | 2.021 | 0.101 | 2.087 | 0.104 | 0.590 | 0.041 | 1.708 | 0.090 |
| 1H-1, 136–138 | 1.37 | 25.5 | 1.941 | 0.096 | 2.174 | 0.105 | 0.594 | 0.040 | 1.724 | 0.089 |
| 1H-1, 146–148 | 1.47 | 27.7 | 1.980 | 0.097 | 2.149 | 0.104 | 0.670 | 0.052 | 1.681 | 0.098 |
| 1H-2, 6–8 | 1.57 | 29.8 | 2.969 | 0.136 | 3.174 | 0.144 | 0.565 | 0.037 | 2.160 | 0.104 |
| 1H-2, 16–18 | 1.67 | 31.9 | 2.155 | 0.109 | 2.379 | 0.119 | 0.582 | 0.040 | 1.766 | 0.093 |
| 1H-2, 26–28 | 1.77 | 34.0 | 2.194 | 0.109 | 2.374 | 0.117 | 0.387 | 0.030 | 1.790 | 0.092 |
| 1H-2, 36–38 | 1.87 | 36.0 | 2.355 | 0.117 | 2.485 | 0.123 | 0.660 | 0.047 | 2.044 | 0.109 |
| 1H-2, 46–48 | 1.97 | 38.1 | 2.163 | 0.104 | 2.387 | 0.113 | 0.493 | 0.034 | 1.756 | 0.086 |
| 1H-2, 56–58 | 2.07 | 40.1 | — | — | — | — | — | — | — | — |
| 1H-2, 66–68 | 2.17 | 42.1 | 2.910 | 0.136 | 3.195 | 0.147 | 0.502 | 0.080 | 2.071 | 0.183 |
| 1H-2, 76–78 | 2.27 | 44.1 | 2.638 | 0.072 | 2.881 | 0.077 | 0.573 | 0.026 | 2.126 | 0.063 |
| 1H-2, 86–88 | 2.37 | 46.2 | 2.743 | 0.129 | 3.028 | 0.140 | 0.553 | 0.039 | 2.211 | 0.109 |
| 1H-2, 96–98 | 2.47 | 48.2 | 3.056 | 0.144 | 3.569 | 0.165 | 0.559 | 0.045 | 2.373 | 0.126 |
| 1H-2, 106–108 | 2.57 | 50.3 | 2.205 | 0.074 | 2.481 | 0.081 | 0.536 | 0.033 | 1.885 | 0.069 |
| 1H-2, 116–118 | 2.67 | 52.3 | 2.234 | 0.080 | 2.287 | 0.082 | 0.532 | 0.027 | 1.804 | 0.061 |
| 1H-2, 126–128 | 2.77 | 54.3 | 2.434 | 0.120 | 2.745 | 0.133 | 0.570 | 0.038 | 1.974 | 0.099 |
| 1H-2, 136–138 | 2.87 | 56.3 | 2.386 | 0.117 | 2.613 | 0.126 | 0.504 | 0.035 | 2.000 | 0.098 |
| 1H-2, 146–148 | 2.97 | 58.4 | 2.066 | 0.109 | 2.262 | 0.116 | 0.652 | 0.042 | 1.859 | 0.086 |
| 1H-3, 6–8 | 3.07 | 60.4 | 1.289 | 0.062 | 1.329 | 0.063 | 0.593 | 0.033 | 1.365 | 0.060 |
| 1H-3, 16–18 | 3.17 | 62.5 | 2.025 | 0.100 | 2.286 | 0.109 | 0.696 | 0.079 | 1.867 | 0.141 |
| 1H-3, 26–28 | 3.27 | 65.1 | 1.869 | 0.080 | 2.105 | 0.088 | 0.522 | 0.031 | 1.643 | 0.070 |
| 1H-3, 36–38 | 3.37 | 67.7 | 3.533 | 0.157 | 3.799 | 0.168 | 0.762 | 0.046 | 2.879 | 0.133 |
| 1H-3, 46–48 | 3.47 | 70.1 | 2.720 | 0.133 | 2.913 | 0.141 | 0.851 | 0.052 | 2.381 | 0.119 |
| 1H-3, 56–58 | 3.57 | 73.2 | 2.854 | 0.128 | 3.193 | 0.141 | 0.559 | 0.036 | 2.554 | 0.117 |
| 1H-3, 66–68 | 3.67 | 76.2 | 2.917 | 0.132 | 3.206 | 0.143 | 0.440 | 0.031 | 2.548 | 0.118 |
| 1H-3, 76–78 | 3.77 | 79.2 | — | — | — | — | — | — | — | — |
| 1H-3, 86–88 | 3.87 | 84.1 | 2.696 | 0.138 | 2.846 | 0.144 | 0.587 | 0.039 | 2.441 | 0.120 |
| 1H-3, 96–98 | 3.97 | 89.0 | — | — | — | — | — | — | — | — |
| 1H-3, 106–108 | 4.07 | 93.5 | 2.241 | 0.119 | 2.448 | 0.129 | 0.444 | 0.033 | 2.055 | 0.109 |
| 1H-3, 116–118 | 4.17 | 98.0 | 2.652 | 0.123 | 2.928 | 0.134 | 0.576 | 0.038 | 2.631 | 0.123 |
| 1H-3, 126–128 | 4.27 | 103.2 | — | — | — | — | — | — | — | — |
| 1H-3, 136–138 | 4.37 | 107.5 | 2.124 | 0.101 | 2.414 | 0.113 | 0.377 | 0.028 | 1.978 | 0.095 |
| 1H-3, 146–148 | 4.47 | 113.1 | — | — | — | — | — | — | — | — |
| 1H-4, 6–8 | 4.57 | 116.8 | 3.559 | 0.170 | 3.822 | 0.180 | 0.532 | 0.036 | 3.469 | 0.157 |
| 1H-4, 16–18 | 4.67 | 119.8 | — | — | — | — | — | — | — | — |
| 1H-4, 26–28 | 4.77 | 122.8 | 3.316 | 0.151 | 3.683 | 0.166 | 0.376 | 0.032 | 3.239 | 0.157 |
| 1H-4, 36–38 | 4.87 | 124.1 | 2.491 | 0.132 | 2.399 | 0.128 | 0.715 | 0.049 | 2.460 | 0.127 |
| 1H-4, 46–48 | 4.97 | 126.0 | 2.019 | 0.127 | 2.108 | 0.131 | 0.634 | 0.061 | 2.130 | 0.250 |
| 1H-4, 56–58 | 5.07 | 127.5 | — | — | — | — | — | — | — | — |
| 1H-4, 66–68 | 5.17 | 129.2 | 2.495 | 0.147 | 2.843 | 0.162 | 0.561 | 0.054 | 2.448 | 0.142 |
| 1H-4, 76–78 | 5.27 | 132.0 | — | — | — | — | — | — | — | — |
| 2H-1, 06–08 | 5.62 | 135.8 | 2.496 | 0.141 | 2.707 | 0.149 | 0.576 | 0.054 | 2.300 | 0.133 |
| 2H-1, 16–18 | 5.67 | 137.1 | — | — | — | — | — | — | — | — |
| 2H-1, 26–28 | 5.77 | 138.2 | 2.040 | 0.128 | 2.137 | 0.132 | 0.597 | 0.057 | 2.060 | 0.130 |
| 2H-1, 36–38 | 5.87 | 140.5 | — | — | — | — | — | — | — | — |
| 2H-1, 46–48 | 5.97 | 142.6 | 2.133 | 0.108 | 2.288 | 0.113 | 0.568 | 0.063 | 1.845 | 0.127 |
| 2H-1, 56–58 | 6.07 | 144.1 | — | — | — | — | — | — | — | — |
| 2H-1, 66–68 | 6.17 | 145.2 | 2.113 | 0.10 | 2.221 | 0.104 | 0.849 | 0.051 | 2.226 | 0.11 |
| 2H-1, 76–78 | 6.27 | 147.6 | 2.095 | 0.10 | 2.227 | 0.110 | 0.864 | 0.050 | 2.154 | 0.11 |
| 2H-1, 86–88 | 6.37 | 149.4 | 2.285 | 0.11 | 2.427 | 0.12 | 0.738 | 0.05 | 2.262 | 0.11 |
| 2H-1, 96–98 | 6.47 | 151.2 | 2.594 | 0.11 | 2.681 | 0.12 | 0.734 | 0.04 | 2.509 | 0.11 |
| 2H-1, 106–108 | 6.57 | 152.7 | 2.426 | 0.12 | 2.495 | 0.12 | 0.718 | 0.05 | 2.338 | 0.12 |
| 2H-1, 116–118 | 6.67 | 154.2 | 2.004 | 0.09 | 2.107 | 0.10 | 0.750 | 0.04 | 2.020 | 0.09 |
| 2H-1, 126–128 | 6.77 | 156.2 | 2.902 | 0.13 | 3.076 | 0.13 | 0.743 | 0.05 | 3.016 | 0.21 |
| 2H-1, 136–138 | 6.87 | 158.0 | 1.989 | 0.10 | 2.174 | 0.11 | 0.840 | 0.05 | 2.123 | 0.11 |
| 2H-1, 146–148 | 6.97 | 159.5 | 2.468 | 0.15 | 2.623 | 0.15 | 0.683 | 0.06 | 2.489 | 0.14 |
| 2H-2, 6–8 | 7.07 | 161.4 | — | — | — | — | — | — | — | — |
| 2H-2, 16–18 | 7.17 | 163.2 | 2.052 | 0.11 | 2.058 | 0.11 | 0.690 | 0.06 | 2.190 | 0.23 |
| 2H-2, 26–28 | 7.27 | 165.0 | 2.461 | 0.12 | 2.782 | 0.13 | 0.591 | 0.05 | 2.332 | 0.12 |
| 2H-2, 36–38 | 7.37 | 166.8 | — | — | — | — | — | — | — | — |
| 2H-2, 46–48 | 7.47 | 168.7 | 2.383 | 0.08 | 2.588 | 0.08 | 0.664 | 0.03 | 2.406 | 0.08 |
| 2H-2, 56–58 | 7.57 | 170.7 | — | — | — | — | — | — | — | — |

**Appendix B (continued).**

| Core, section, interval (cm) | Depth (mbsf) | [a]Age (k.y.) | $^{238}U$ (dpm $g^{-1}$) | ± | $^{234}U$ (dpm $g^{-1}$) | ± | $^{232}Th$ (dpm $g^{-1}$) | ± | $^{230}Th$ (dpm $g^{-1}$) | ± |
|---|---|---|---|---|---|---|---|---|---|---|
| 117-722B- (Cont.) | | | | | | | | | | |
| 2H-2, 66–68 | 7.67 | 172.8 | 2.145 | 0.11 | 2.290 | 0.11 | 0.622 | 0.06 | 1.998 | 0.12 |
| 2H-2, 76–78 | 7.77 | 175.2 | — | — | — | — | — | — | — | — |
| 2H-2, 86–88 | 7.87 | 177.6 | 3.068 | 0.14 | 3.253 | 0.15 | 0.755 | 0.08 | 3.216 | 0.19 |
| 2H-2, 96–98 | 7.97 | 180.0 | — | — | — | — | — | — | — | — |
| 2H-2, 106–108 | 8.07 | 182.0 | 2.265 | 0.12 | 2.408 | 0.13 | 0.589 | 0.05 | 2.283 | 0.13 |
| 2H-2, 116–118 | 8.17 | 184.1 | — | — | — | — | — | — | — | — |
| 2H-2, 126–128 | 8.27 | 186.2 | 2.096 | 0.12 | 2.327 | 0.13 | — | — | — | — |
| 2H-2, 136–138 | 8.37 | 187.7 | — | — | — | — | — | — | — | — |
| 2H-2, 146–148 | 8.47 | 189.7 | 1.704 | 0.06 | 2.137 | 0.07 | — | — | — | — |
| 2H-3, 06–08 | 8.57 | 191.1 | — | — | — | — | — | — | — | — |
| 2H-3, 16–18 | 8.67 | 193.2 | 2.037 | 0.10 | 2.123 | 0.11 | — | — | — | — |
| 2H-3, 26–28 | 8.77 | 197.6 | — | — | — | — | — | — | — | — |
| 2H-3, 36–38 | 8.87 | 200.8 | 2.335 | 0.10 | 2.447 | 0.10 | 0.313 | 0.02 | 2.320 | 0.10 |
| 2H-3, 46–48 | 8.97 | 204.3 | — | — | — | — | — | — | — | — |
| 2H-3, 56–58 | 9.07 | 208.0 | 1.351 | 0.05 | 1.475 | 0.07 | 0.592 | 0.03 | 1.567 | 0.06 |
| 2H-3, 66–68 | 9.17 | 211.5 | — | — | — | — | — | — | — | — |
| 2H-3, 76–78 | 9.27 | 215.0 | 2.390 | 0.11 | 2.470 | 0.11 | 0.664 | 0.04 | 2.496 | 0.10 |
| 2H-3, 86–88 | 9.37 | 218.5 | — | — | — | — | — | — | — | — |
| 2H-3, 96–98 | 9.47 | 222.1 | 3.121 | 0.16 | 3.376 | 0.17 | 0.636 | 0.04 | 2.524 | 0.13 |
| 2H-3, 106–108 | 9.57 | 225.8 | — | — | — | — | — | — | — | — |
| 2H-3, 116–118 | 9.67 | 229.8 | 2.700 | 0.14 | 2.850 | 0.15 | 0.524 | 0.04 | 2.781 | 0.13 |
| 2H-3, 126–128 | 9.77 | 233.4 | — | — | — | — | — | — | — | — |
| 2H-3, 136–138 | 9.87 | 237.0 | 1.799 | 0.13 | 2.016 | 0.14 | 0.337 | 0.03 | 2.010 | 0.09 |

[a] Stratigraphy from Clemens and Prell, pers. comm., March 1989.
— Sample not analyzed.